IEEE Access
Multidisciplinary ⋮ Rapid Review ⋮ Open Access Journal

Received 9 January 2024, accepted 15 January 2024, date of publication 19 January 2024, date of current version 25 January 2024.

Digital Object Identifier 10.1109/ACCESS.2024.3356355

RESEARCH ARTICLE

MTPA Speed Control for IPMSM Drives Without Current Sensing

ALAREF ELHAJ[1], MOHAMAD ALZAYED[1], (Member, IEEE), AND HICHAM CHAOUI[1,2], (Senior Member, IEEE)

[1]Intelligent Robotic and Energy Systems Research Group (IRES), Department of Electronics, Carleton University, Ottawa, ON K1S 5B6, Canada
[2]Department of Electrical and Computer Engineering, Texas Tech University, Lubbock, TX 79409, USA

Corresponding author: Mohamad Alzayed (mohamad.alzayed@carleton)

ABSTRACT This paper introduces a current sensorless speed control method for interior permanent magnet synchronous motors (IPMSMs) to track the maximum torque per ampere (MTPA) trajectory. Unlike traditional cascaded control structures, current measurements and inner regulation loops are eliminated. Instead, the MTPA is attained by directly adjusting the voltage vector amplitude and angle. An analytical formulation based on the motor voltage model is developed to extract the optimal voltage amplitude to run the motor within the MTPA operating points, disregarding any control law approximation or lookup tables-based numerical solutions. As a result of excluding current measurements and regulation loops, a one-speed controller is required. This leads to a significant reduction in control system complexity. Moreover, the simple structure of the control system highly qualifies it for cost-effective implementation of IPMSM applications. The validity of the designed control method is confirmed experimentally using a 5*Hp* IPMSM. The experimentally obtained results are compared to the conventional field-oriented MTPA (FOC) to highlight the effectiveness of the suggested control system considering different operating conditions. Additionally, the MTPA trajectory tracking accuracy is quantitatively assessed using two performance metrics.

INDEX TERMS Interior permanent magnet synchronous motor (IPMSM), current sensorless, maximum torque per ampere (MTPA), direct voltage control.

I. INTRODUCTION

Interior permanent magnet synchronous motors (IPMSMs) are constantly expanding their application areas and increasingly permeating various industries that were dominated by other motors [1], [2], [3]. Thanks to their unique features, such as high power density, high torque production, high efficiency, and the capability of running at a wide constant power operating range [4], IPMSMs have drawn considerable research interest and are widely employed in various applications such as electric vehicles, servo drives traction systems, etc [5]. In addition to magnetic torque produced by the permanent magnets (PMs), IPMSM also produces a reluctance torque as a result of the embedded arrangement of the PMs [6], [7]. This denotes that the direct and quadratic axis stator currents share the torque production of the IPMSM. The special rotor configuration with buried PMs gives the opportunity for the saliency effect to present, resulting in a greater q-axis inductance compared to the d-axis inductance [8]. Thus, a cross-magnetization phenomenon will be generated as a result of this inequality because of the interaction between the direct and quadratic currents. Along with cross-magnetization, several additional factors, including magnetic saturation and temperature change, cause an increase in the motor's non-linearity [9]. Thus, it is challenging to regulate the IPMSM's speed accurately [10]. To adopt an efficient IPMSM drive system, an adequate current control procedure is essential to precisely extract the d–q axes currents and develop the desired electromagnetic torque [11], [12]. Because of its ability to achieve maximum torque with minimum current consumption, maximum torque per ampere control (MTPA)

The associate editor coordinating the review of this manuscript and approving it for publication was Alfeu J. Sguarezi Filho.

is the most widely used control strategy that can satisfy the aforementioned requirements.

Several approaches have been investigated to enhance the MTPA tracking accuracy at a wide range of speed and torque. The fundamental concept of these control techniques is to force the system's operating point to lie within the MTPA trajectory, ensuring high torque production with less current usage and reduced copper losses [13]. A model-based MTPA control is studied in [12]. In the study, the current components are extracted based on the differentiation of the electromagnetic torque equation with respect to the angle of the current vector and setting it to null [14]. In [15], the MTPA points are obtained using lookup tables (LUT). These tables are used to create the required reference currents for the MTPA. The generation of LUT depends on the data collected after establishing several offline tests under different disturbances, such as load and speed changes [16]. However, creating these lookup tables consumes considerable time and uses more memory space [9].

Recently, various MTPA strategies based on signal injection have been addressed. The MTPA points are detected by injecting a current or voltage signal into the IPMSM. The injected signal could be actual or virtual [17]. In [18], the MTPA points are extracted after injecting a current signal with high frequency into the machine and equating the torque derivative to zero. However, injecting a high-frequency current signal causes torque and speed ripple [13].

It is well known that analytical MTPA approaches, such as field-oriented control (FOC), use cascaded control loops to indirectly extract the required reference voltages to drive the motor within the MTPA trajectory [19]. However, such control strategies need multiple proportional-integral (PI) regulators in their control loops. As a result, excessive gain-tuning is required for optimal control signals. This results in significant time costs in practical applications and burdens the overall control performance [20].

In an attempt to simplify the MTPA control structures that use cascaded loops for current regulation and reduce the tuning time associated with them, a direct voltage MTPA control for IPMSM has been investigated in [21], [22], [23], [24], [25], [26], and [27]. In these strategies, the MTPA is achieved by directly modifying the voltage vector amplitude and angle, eliminating the use of current regulation loops and the current sensors in sensorless methods. This significantly reduces the control scheme's complexity and the time required for tuning [21]. Heretofore, the few developed direct voltage control methods still need current sensors [22], [23], inner stabilizing loops [24], or their control laws are derived based on long-winded iterative calculations or numerical approximation [25], [26], [27]. Considering the transient states, a direct voltage MTPA without current sensing is implemented in [25] to enhance the control system's performance. As a transition to a sensorless technique, the current components are calculated from the motor's electrical model and directly injected into the control loop, which may exhibit a significant noise in the absence of any estimator [28]. Furthermore, the control signals are extracted based on long-winded calculations followed by many iterations to reach the optimum values, increasing the computational burden of the control system. A simple current sensorless direct voltage MTPA strategy is presented in [26]. Although this method offers a simple control structure and fast transient response, it still relies on the numerical approximation of its control law, where the voltage amplitude is introduced as a function of motor speed and voltage angle, in addition to numerically approximated control coefficients, which requires excessive tuning to reach the optimal operating points as a response to various uncertainties. Furthermore, the MTPA trajectory tracking can not be ensured in all operation ranges because the tuning process is not straightforward. At the expense of extensive computation, an alternative is introduced in [27]. However, the voltage amplitude is calculated numerically, and the obtained offline results are stored in a lookup table.

This article presents a simple current sensorless maximum torque per ampere control strategy for IPMSM. The proposed method relies only on adjusting the voltage vector amplitude and angle with the aid of a single PI controller. Unlike the previously developed direct voltage MTPA methods, the designed strategy provides a complete formulation based on machine voltage equations to derive the MTPA voltage amplitude analytically, disregarding any control law approximation or lookup tables-based numerical solutions. The strength of the designed strategy lies in its analytically derived voltage amplitude control law. Firstly, calculating the voltage amplitude directly from the motor's electrical model, excluding any numerical or iterative solution, enhances the control system's computation efficiency. Secondly, the voltage amplitude control law is analytically decided and addressed as a function of speed and motor electrical parameters. Therefore, the MTPA trajectory tracking can be guaranteed in all operating ranges since it does not need further control coefficient tuning. Consequently, a direct and uncomplicated control system is developed. Furthermore, the easiness of its tuning and straightforward implementation. This makes the proposed strategy a promising alternative for cost-effective real-time implementation.

The remainder of this manuscript is structured as follows: Section II explains the IPMSM's dynamics. Section III is a detailed description of the proposed model. The experimental results are displayed and discussed in Section IV.

II. IPMSM *D–Q* MODEL

In the rotating synchronous reference frame, the electrical and the mechanical representations of the interior permanent magnet synchronous motor IPMSM can be illustrated as follows [29]:

$$v_d = Ri_d + L_d \frac{d}{dt} i_d - L_q \omega_e i_q \tag{1a}$$

$$v_q = Ri_q + L_q \frac{d}{dt} i_q + L_d \omega_e i_d + \lambda \omega_e \tag{1b}$$

$$T_e = \frac{3}{2}p[(L_d - L_q)i_d i_q + \lambda i_q] \tag{1c}$$

The motion's mechanical equations are described by:

$$\frac{d}{dt}\omega = \frac{1}{J}(T_e - T_F - T_L) \tag{2a}$$

$$\frac{d}{dt}\theta = p\omega \tag{2b}$$

where, v_d, v_q are the stator voltages and i_d, i_q are the direct and quadratic stator currents, L_d, L_q are the direct and quadratic inductance, R is the resistance of stator windings, λ is the flux linkage of PMs, ω_e and ω are the electrical and mechanical speed of the motor shaft, p is the number of pole pairs, J is the inertia, θ is the motor's shaft electrical angle, and T_e, T_L, and T_F are electromagnetic, load, and friction torques, respectively. To avoid the system's complexity, the effect of friction torque is represented by the relation between the coefficient of viscosity and the motor's angular speed $T_F = F\omega$, where F is the viscous friction coefficient, which is considered as a lumped representative of the nonlinear terms of friction torque [30].

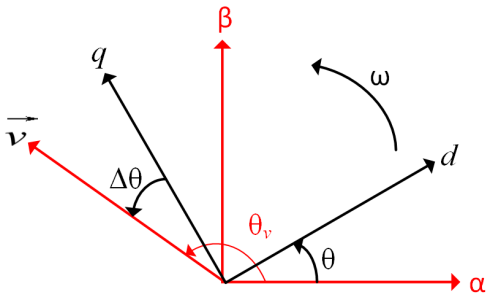

FIGURE 1. The mapping of the applied voltage vector in regard to the stationary and rotating frames.

According to the d–q coordinates of the voltage vector shown in Fig. 1, the voltage vector's amplitude and angle (v, $\Delta\theta$) can be constructed as follows:

$$v = \sqrt{(v_d)^2 + (v_q)^2} \tag{3}$$

$$\Delta\theta = -\tan^{-1}\left(\frac{v_d}{v_q}\right) \tag{4}$$

where $\Delta\theta$ represents the angle between the voltage vector and the quadratic axis.

III. DIRECT VOLTAGE MTPA CONTROL

Direct voltage MTPA control involves generating the intended torque with a minimum current consumption by directly controlling the applied voltage vector magnitude and angle (v, $\Delta\theta$). Whenever an external load torque is applied to the IPMSM, the motor generates an electromagnetic torque in reaction to the applied one. The generated torque is mainly determined by the motor's drawn current, which relies on the separation angle between the excitation voltage and the motor's internal voltage. Therefore, proper and precise voltage amplitude and angle control results in optimized current consumption and speed regulation.

The main purpose of this research is to develop a current sensorless control system for the interior permanent magnet synchronous motor to achieve the MTPA while matching the measured speed (ω) with the predefined reference speed (ω^*). Since there are unlimited possibilities of (v, $\Delta\theta$) that can produce a given torque and speed, this strategy seeks to identify the optimal combination of v and $\Delta\theta$ to develop the desired torque with less current usage. Having the ability to measure the motor speed and compare it to the reference speed, we can define the speed error as the difference between the commanded and actual speed $e_\omega = \omega^* - \omega$. The obtained error is fed into a PI controller, which drives it to zero and generates the optimum voltage angle $\Delta\theta$, which is needed to produce the required voltage amplitude to drive the motor within the MTPA limits. The rationale behind adopting a PI controller is due to its simplicity, accurate steady-state performance, and straightforward real-time implementation. Furthermore, a PI-type controller eliminates the need to deal with derivative action and its associated challenges, such as noise amplification and sensitivity to high-frequency noise.

Therefore, the voltage angle control law can be written as,

$$\Delta\theta = K_p e_\omega + K_i \int e_\omega \tag{5}$$

where K_p and K_i are the gains of the PI regulator that are selected using empirical study, and e_ω is the speed error.

In the absence of current measurements and regulation loops, the reference voltage amplitude (v^*) is represented as a feed-forward term in the control system structure (see Fig. 2). This term is derived analytically from the motor's voltage equations as follows:

Assuming the motor is running under steady-state conditions, (1a), (1b) can be addressed as [31]:

$$v_d = Ri_d - L_q\omega_e i_q \tag{6a}$$

$$v_q = Ri_q + L_d\omega_e i_d + \lambda\omega_e \tag{6b}$$

Substituting (6a), (6b) in (3), (4) leads to,

$$v = \sqrt{\begin{array}{c}(Ri_d)^2 - 2(RL_q i_d i_q \omega_e) + (L_q\omega_e i_q)^2 + (Ri_q)^2 \\ +2Ri_q(L_d i_d + \lambda)\omega_e + ((L_d i_d + \lambda)\omega_e)^2\end{array}} \tag{7}$$

$$\Delta\theta = -\tan^{-1}\left(\frac{Ri_d - L_q\omega_e i_q}{Ri_q + L_d\omega_e i_d + \lambda\omega_e}\right) \tag{8}$$

Neglecting the voltage drop due to armature winding resistance, the voltage amplitude and angle becomes [23]:

$$v = \sqrt{(L_q\omega_e i_q)^2 + \omega_e^2(L_d i_d + \lambda)^2} \tag{9}$$

$$v = \omega_e\sqrt{L_q^2 i_q^2 + L_d^2 i_d^2 + 2L_d i_d\lambda + \lambda^2} \tag{10}$$

$$\Delta\theta = \tan^{-1}\left(\frac{L_q i_q}{L_d i_d + \lambda}\right) \tag{11}$$

In [32] and [33], the i_d current required for achieving the maximum torque per ampere operation point is expressed as,

$$i_d = \left(\frac{L_d - L_q}{\lambda}\right) i_q^2 \tag{12}$$

Using the MTPA current equation (12) to mathematically derive the required voltage amplitude for the MTPA forces the PI controller to produce the optimum angle.

Substituting (12) in (10) leads to,

$$v = \omega_e \sqrt{L_q^2 i_q^2 + [L_d^2 (\frac{L_d - L_q}{\lambda})^2 i_q^4 + 2\lambda L_d (\frac{L_d - L_q}{\lambda}) i_q^2 + \lambda^2} \tag{13}$$

The term $\left(\frac{L_d - L_q}{\lambda}\right)$ in (13), which involves the inductance difference divided by the flux linkage, has a small value $\ll 1$. In addition, it is squared and multiplied by L_d^2. This makes its contribution to the voltage equation very small. Thus, the high order terms can be neglected, $\left(\frac{L_d - L_q}{\lambda}\right)^2 i_q^4 \approx 0$. Therefore, the voltage amplitude can be written as,

$$v = \omega_e \sqrt{(L_q^2 + 2L_d(L_d - L_q)) i_q^2 + \lambda^2} \tag{14}$$

At this point, the voltage amplitude is still based on the measured quadratic component of stator current (i_q). Taking advantage of speed controller output ($\Delta\theta$), the voltage amplitude can be constructed without the need for current measurement.

Using (11) and (12), the voltage angle can be addressed as follows:

$$\Delta\theta = \tan^{-1}\left(\frac{L_q i_q}{L_d (\frac{L_d - L_q}{\lambda}) i_q^2 + \lambda}\right) \tag{15}$$

$(\frac{L_d - L_q}{\lambda})$ in (15) holds a small value $\ll 1$ [34]. In addition, it is multiplied by L_d, which makes it very small. Therefore, the contribution of $L_d(\frac{L_d - L_q}{\lambda})$ to the equation can be neglected even in the case of load increase conditions when the value of i_q will increase because the term holds a very small value. Furthermore, in real-time, the value of the electrical parameters (L_d, L_q, λ) decreases as the motor's current increases [35], [36]. Thus, $L_d(\frac{L_d - L_q}{\lambda}) \approx 0$.

$$\Delta\theta = \tan^{-1}\left(\frac{L_q i_q}{\lambda}\right) \tag{16}$$

Since ($\Delta\theta$) is decided by the speed regulator, (16) can be reconstructed as,

$$i_q = \frac{\lambda}{L_q} \tan(\Delta\theta) \tag{17}$$

Substituting (17) in (14) yields voltage amplitude as a function of (ω, $\Delta\theta$), in addition to machine electrical parameters (L_d, L_q, λ). Thus, MTPA control is achieved analytically without the need for current measurement.

$$v = \omega_e \sqrt{\lambda^2 + [\frac{L_q^2 + 2L_d(L_d - L_q)}{L_q^2}]\lambda^2 \tan^2(\Delta\theta)} \tag{18}$$

The reference voltage amplitude equation can be written as,

$$v^* = \omega_e^* \sqrt{K_{v_1} + K_{v_2} \tan^2(\Delta\theta)} \tag{19}$$

where,

$$K_{v_1} = \lambda^2 \tag{20}$$

$$K_{v_2} = \lambda^2 \left(\frac{L_q^2 + 2L_d(L_d - L_q)}{L_q^2}\right) \tag{21}$$

The coefficients K_{v_1}, K_{v_2} are calculated based on the nominal values of flux linkage, direct inductance, and quadratic inductance (λ, L_d, L_q), respectively.

The applied voltage to the motor can be given as follows:

$$v^*_{\alpha\beta} = v^* \angle \theta_v \tag{22}$$

$$\theta_v = \Delta\theta + \theta + \frac{\pi}{2} \tag{23}$$

where v^* defines the voltage amplitude, θ_v represents the angle between the α-axis and the applied voltage vector, and θ is the rotor position, as seen in Fig 1.

Lastly, the applied voltage is transformed to a Cartesian form and fed to space vector pulse width modulation (SVPWM) to generate a proper duty cycle for the inverter, as shown in Fig. 2

During the derivation process of the voltage amplitude control law, certain measures of reduction are utilized to reduce the control system's complexity. Therefore, further study is conducted to assess the simplicity of the proposed strategy, as these assumptions may affect the other operation characteristics of the motor. In this study, the voltage amplitude is addressed with respect to speed and load torque for the adopted simplified control law (19) and the complex approach (7) before simplification. Fig. 3 displays the surface plot of the voltage amplitude using the adopted simplified strategy against the non-simplified approach. As observed, both surfaces show good coincidence. Thus, the validity of the proposed simplified voltage amplitude control law is confirmed.

IV. EXPERIMENTAL RESULTS AND DISCUSSION

A. SETUP

A 3.7 kW/5Hp, 1800rpm IPMSM is employed experimentally to examine the effectiveness of the designed direct voltage MTPA control strategy. The IPMSM parameters are given in Table 1. To ensure accurate validation, an experimental parameter measurement according to the room temperature is conducted prior to the experiment, where the machine parameters (R, L_d, L_q and λ) from the motor's datasheet are adjusted according to the measured values. In the real-time test, an IGBT-based inverter of 10 kW is used to run the IPMSM in a speed mod coupled with an induction motor with the same output power to provide the required load torque. 350 V_{dc} is fed to the inverter from a Magna-Power XR 375 DC power supply, which is equipped with a current limiter to protect the motor and other devices against overcurrent. 20 kHz and 4 kHz are used as sampling and switching frequencies, respectively. The actual rotor position is acquired with the help of a pulse encoder with a resolution of 1024 pulse/rotation. The model is developed

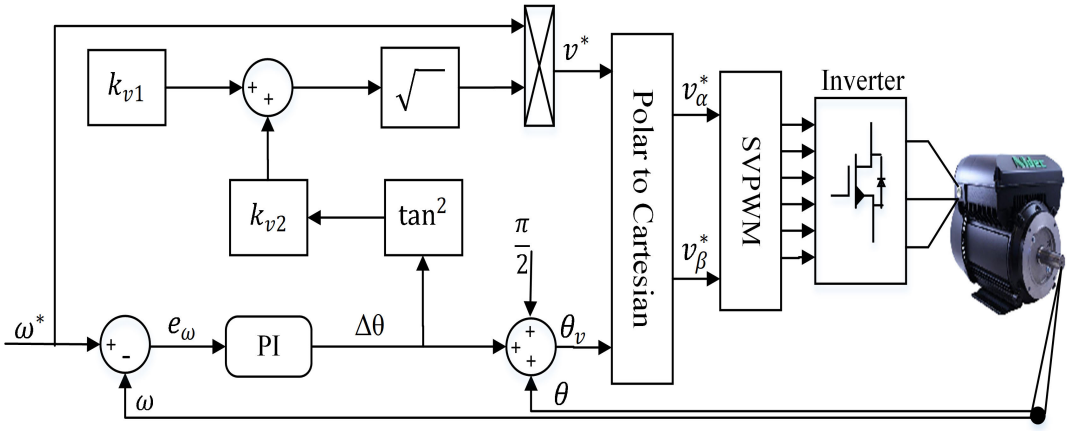

FIGURE 2. Schematic representation of the designed direct voltage MTPA.

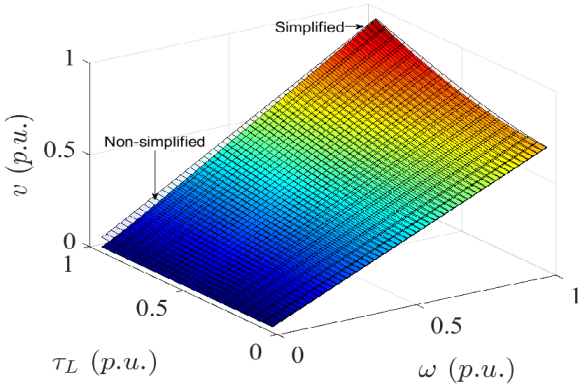

FIGURE 3. Surface plot of the voltage amplitude using simplified and non-simplified control law.

TABLE 1. IPMSM parameters.

Parameter	Symbol	Value
Rated power	P	5 Hp
Rated speed	ω	1800 RPM
Rated torque	T	19.8 N.m
Rated voltage	v	230 V
Flux linkage	λ	$10.8.10^{-}2$ Wb
Pole pairs	p	3
Direct axis inductance	L_d	4.2 mH
Quadratic axis inductance	L_q	8.3 mH
Resistance of stator winding	R	0.2 Ω
Viscous friction coefficient	F	$1.5.10^{-}2$ N· m· s/rad

in MATLAB/Simulink. TMS320F28379D DSP is integrated with MATLAB/Simulink to provide an interface with the experimental setup.

B. EXPERIMENTAL RESULTS

The widely recognized field-oriented MTPA control (FOC) is used as a benchmark to evaluate the effectiveness of the conducted direct voltage control. The main idea behind the comparison is to investigate the MTPA operating points and to demonstrate that the proposed control strategy tracks the MTPA under the same operating conditions as the FOC. The IPMSM is controlled using the proposed strategy, and then FOC is used for comparison. The results are shown in Fig. (4, 5, 6, 7, 8, 9). In these experiments, three scenarios are adopted. In the three scenarios, the user-defined reference and measured speeds are passed through a critically damped second-order filter to reduce noise, smooth the signal, enhance system stability, and adapt the reference speed as needed.

Firstly, in both cases of FOC and direct voltage, the reference speed is started from zero and then stepped up to its rated value of 1800 rpm at $t = 4$ s and then the same speed until $t = 24$ s, when the speed is brought back to its initial value of zero as depicted in Figs. 4(a) and 5(a). At steady state, 19.8 N.m external load torque is introduced to the machine at $t = 9$ s for 10 s and then released at $t = 19$ s. As revealed, both methods show perfect speed tracking under nominal conditions. Fig. 4(a) shows the ability of the designed strategy to track the rated value of the reference speed, demonstrating the controller's capability of regulating the voltage angle as compensation for the speed deviation while maintaining an acceptable current consumption. However, as the load torque goes into effect, a remarkable momentary speed deviation is observed, but the controller compensates for it by delivering an adequate voltage angle. Taking into account that avoiding the current sensing would cause excessive current consumption, the proposed control scheme has demonstrated its capability to handle the sudden load torque presence with a current consumption of about 16 A, which is comparable to the consumed current using FOC, as shown in Figs. 4(b), 5(b). This demonstrates that the motor is working within an acceptable MTPA operating point without the need for current measurement and regulation. Figs. 4(c), 5(c) show the (rms) value of stator current. It is observed that both control methods exhibit a slight current overshoot during the acceleration and at the beginning of the loading period. Although the proposed method exhibits a higher overshoot,

the current attained the desired steady state faster. This is attributed to the fact that direct voltage control uses a single control loop, while FOC adopts cascaded control loops. The overall performance of the designed scheme can be summarized in Fig. 4(d), which shows the advantages of using a single PI controller to regulate the voltage angle directly and how it acts rapidly as a response to sudden speed and torque changes, eliminating the delays associated with cascaded structures of the traditional MTPA FOC, as shown in Fig. 5(d).

In the second scenario, the performance of the proposed control is evaluated under different speed values. Hence, more experiments are conducted, and the results are expressed in Figs. 6, 7. In this scenario, the speed is set to start from zero and then stepped up to 1000 rpm at t = 4 s, continuing at the same level for 5s, and then dropped suddenly to 500 rpm at $t = 14$ s. At $t = 24$ s, a sudden increase occurred to reach 1500 rpm and then gradually dropped to (1100, 800, and 400) rpm at (34 s, 44 s, and 54 s) respectively, as seen in Figs. 6(a), 7(a). A 10 N.m external load torque is introduced at $t = 10$ s and then released at $t = 60$ s. These conditions are applied to the two control methods. Figs. 6(a), 7(a) show that both strategies offer good tracking performance. Since the objective of the MTPA control is to achieve maximum torque with minimum current consumption, the amount of consumed current using the proposed method, to some extent, is comparable to that of the FOC, as depicted in Figs. 6(b), 7(b). During the loading period, Fig. 6(d) shows the controller's capability to respond quickly to sudden changes in speed by changing the voltage angle and amplitude. The designed control scheme has demonstrated that obtaining the optimum $\Delta\theta$ would contribute to the required voltage for torque compensation and current consumption.

In the last scenario, the motor is operated at 1500 rpm, starting at $t = 5$ s and ending at $t = 55$ s. An external load torque of 5 N.m is applied at $t = 10$ s and then stepped up by five every 10 s to reach its rated value and released at $t = 50$ s. The obtained results are expressed in Figs. 8, 9. Figs. 8(a), 9(a) show good speed tracking for both methods, with the ability of the proposed control method to track the reference speed with almost the same current consumption compared to the FOC strategy, as shown in Figs. 8(b), 9(c). In response to the sudden load changes, the current attained the steady state faster in the current sensorless approach, referring to the fact that the designed strategy uses a single control loop that directly controls the amplitude and the angle of the applied voltage vector. Fig. 8(d) shows the compensation that was made by the speed controller for any step increase in the load and, hence, the voltage amplitude to keep the motor running at the required speed, which is considered the main contribution of the designed strategy.

It is well known that the motor's electrical parameters (R, L_d, L_q, λ) are time-varying where motor inductance varies with current while flux linkage and ohmic resistance vary with temperature [37], [38]. Therefore, a simulation study

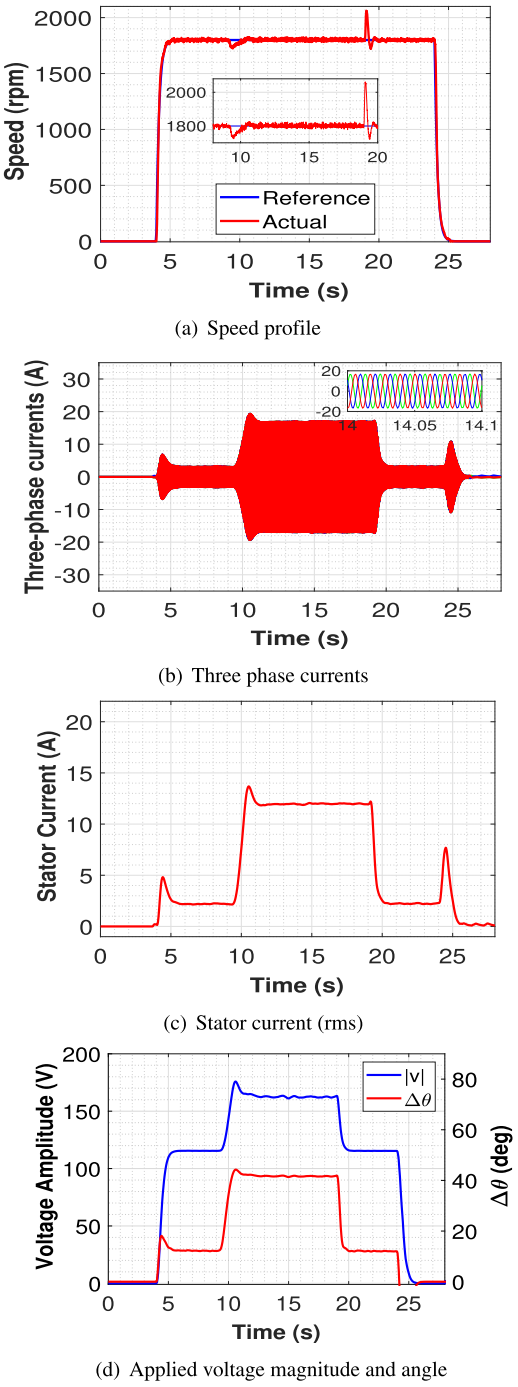

(a) Speed profile

(b) Three phase currents

(c) Stator current (rms)

(d) Applied voltage magnitude and angle

FIGURE 4. Experimental results of the proposed MTPA under rated speed and torque.

is conducted to investigate the capability of the proposed controller to withstand various parametric uncertainties. At rated speed and load conditions, the motor's electrical parameters (R, L_d, L_q, and λ) are adjusted by $\pm$ 20% of their nominal values (Table 1) at time intervals between (25–40 s, 50–65 s, 75–90 s, 95–110 s), respectively. The designed controller's performance under parameters perturbation is depicted in Fig. 10. As revealed, the proposed method

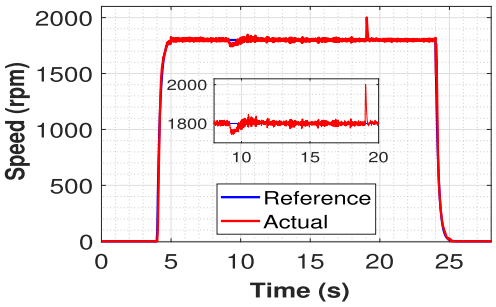

(a) Speed profile

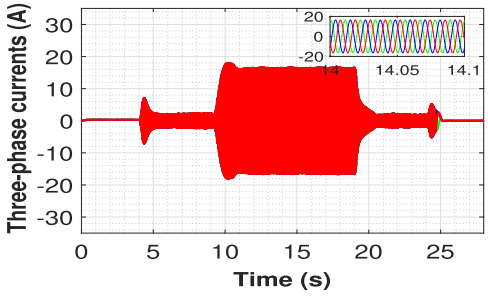

(b) Three phase currents

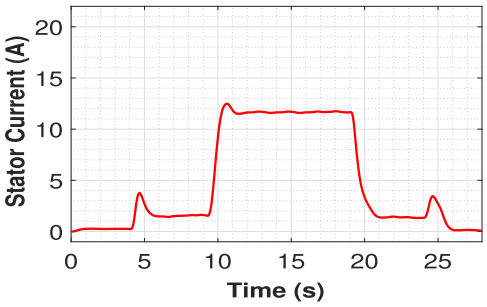

(c) Stator current (rms)

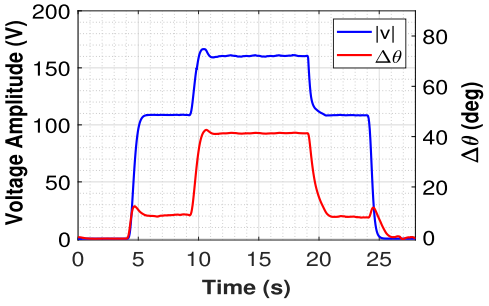

(d) Applied voltage magnitude and angle

FIGURE 5. Experimental results of MTPA FOC under rated speed and torque.

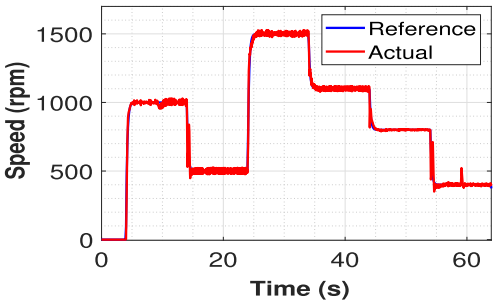

(a) Speed profile

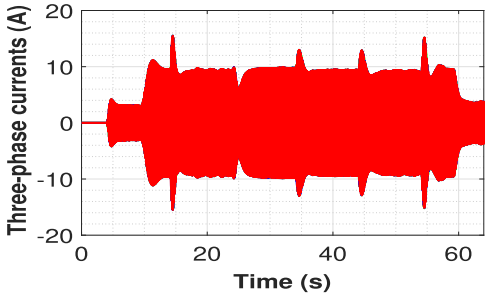

(b) Three phase currents

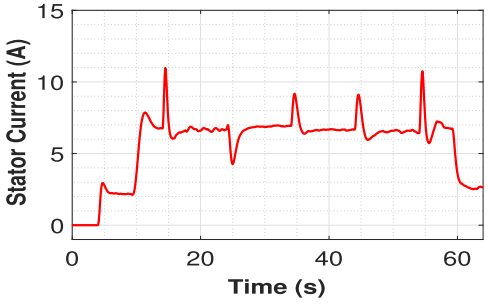

(c) Stator current (rms)

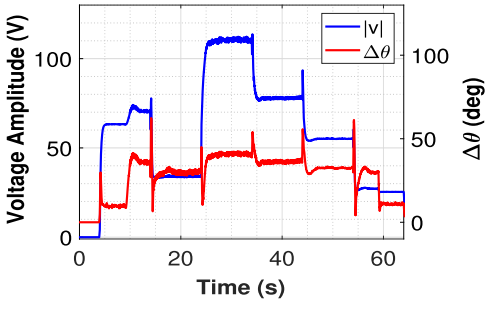

(d) Applied voltage magnitude and angle

FIGURE 6. Experimental results of the proposed MTPA under 10 N.m and variable speed profile.

can deal successfully with the variation of R, L_d, and to some extent L_q, where the speed error during the variation stays within the range of 1 rpm, as shown in Fig. 10(a). Furthermore, the current consumption is almost the same as the current consumption under nominal values, as shown in Figs. 10(b), 10(c). This denotes that the designed strategy can regulate the motor's speed to its reference value even in the case of these variations. On the other hand, the proposed strategy exhibits more sensitivity to flux (λ) variations. This sensitivity is expected because the permanent magnet flux is the most dominant term in the voltage amplitude control law (19). Generally, acceptable performance is achieved even in the case of $\pm$ 20% flux variation, which leads to a speed error of about 11 rpm 0.6% of the reference speed. Fig. 10(d) shows the control signals (v, $\Delta\theta$) and how they compensate for parameter variation.

To further investigate the effect of parameter variation on the proposed method performance, a sensitivity analysis

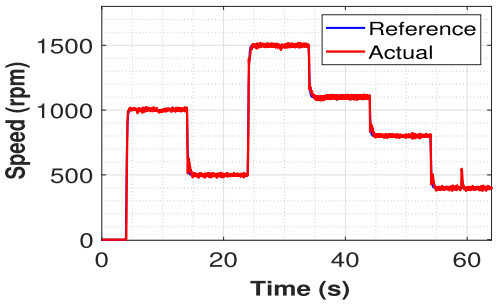

(a) Speed profile

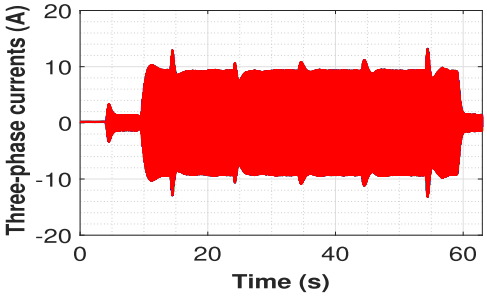

(b) Three phase currents

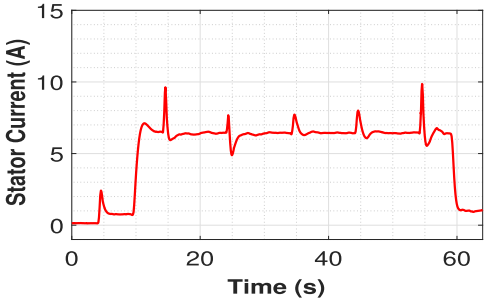

(c) Stator current (rms)

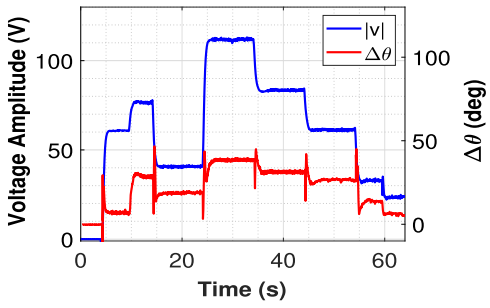

(d) Applied voltage magnitude and angle

FIGURE 7. Experimental results of MTPA FOC under 10 N.m and variable speed profile.

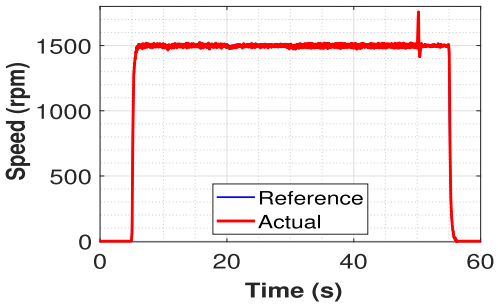

(a) Speed profile

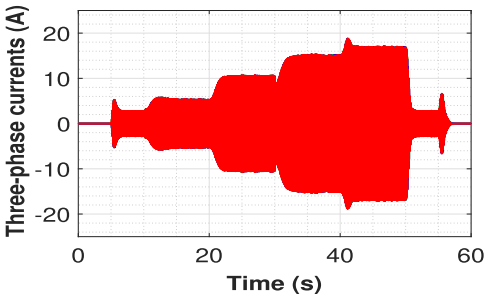

(b) Three phase currents

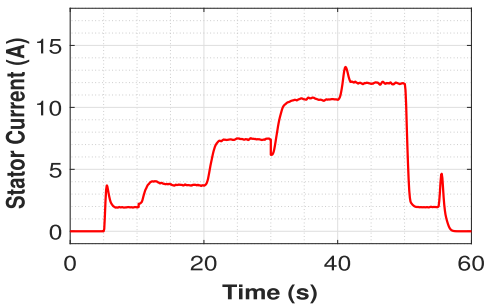

(c) Stator current (rms)

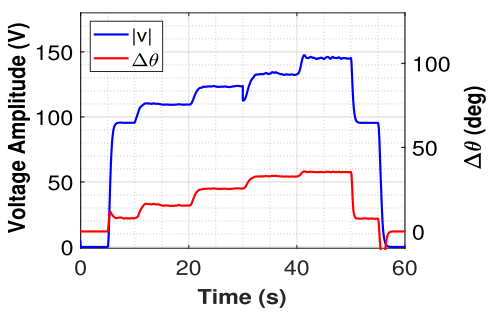

(d) Applied voltage magnitude and angle

FIGURE 8. Experimental results of the proposed MTPA under step increased torque and 1500 RPM.

is conducted using the sensitivity function (S_f^p) addressed in [39]. It is defined as the ratio between the relative variation of a function f and the relative variation of the system's parameter p. Therefore, the sensitivity function can be written as:

$$S_f^p = \frac{df}{dp}\frac{p}{f} \tag{24}$$

The sensitivity investigation is carried out under ± 20% change in (R, L_d, L_q, and λ), and the results are expressed in Table 2.

In the parameters sensitivity analysis, as the sensitivity function approaches zero, the less the system performance is influenced by parameter change. From Table 2, it can be inferred that the system sensitivity to parameter variation is very low for R, L_d, L_q and acceptable for λ.

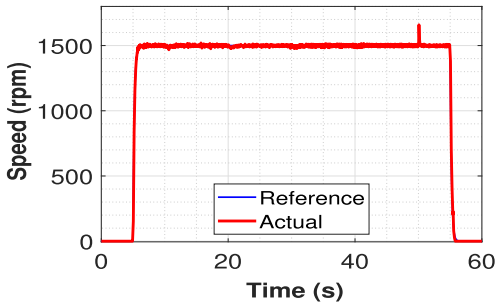

(a) Speed profile

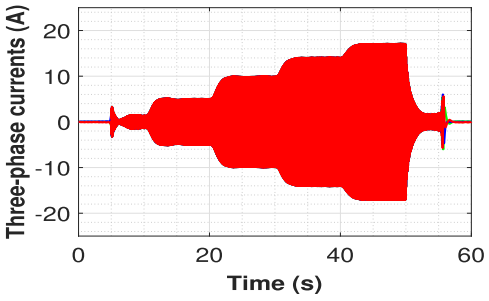

(b) Three phase currents

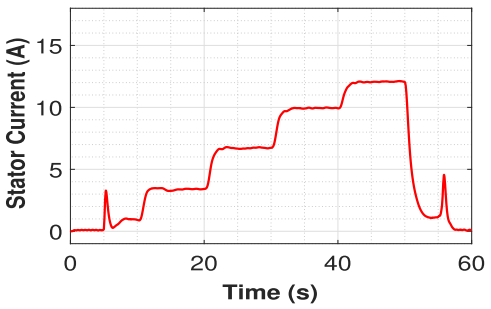

(c) Stator current (rms)

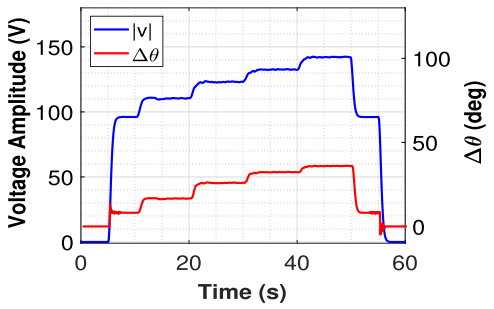

(d) Applied voltage magnitude and angle

FIGURE 9. Experimental results of FOC under step increased torque and 1500 RPM.

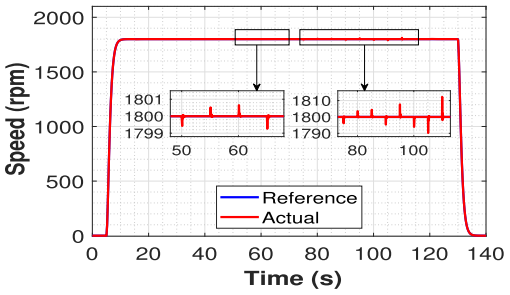

(a) Speed profile

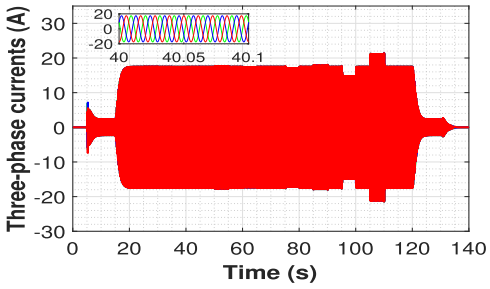

(b) Three phase currents

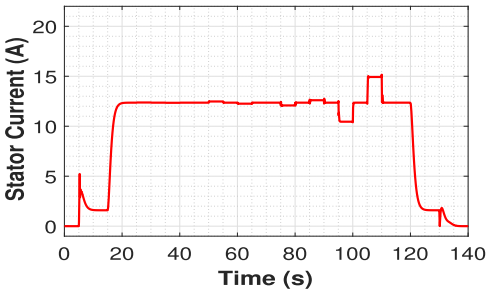

(c) Stator current (rms)

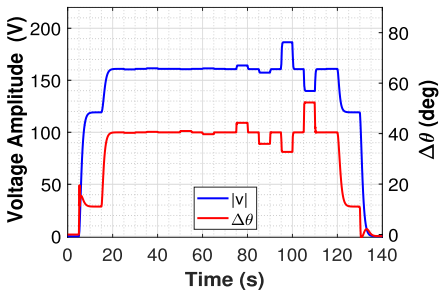

(d) Applied voltage magnitude and angle

FIGURE 10. Evaluation results of the proposed MTPA under parameters variation.

Next, the proposed controller's performance is evaluated under a magnified viscous friction coefficient. Under nominal speed and at t = 30 s, a three times magnified viscous friction coefficient is unexpectedly introduced to the IPMSM. In Fig. 11, the controller's ability to compensate for friction uncertainties is demonstrated. Despite the unexpected increase, the controller effectively regulates the motor's speed to its rated value with a slight deviation of 8 rpm, which is only about 0.4% of the reference speed as depicted in Fig. 11(a). As expected, Fig. 11(b) shows a higher current utilization because of the increased friction. Fig. 11(c) shows the compensation made by control signals (v, $\Delta\theta$) as a response to friction increase.

Considering the field-oriented MTPA control (FOC) as a benchmark, a performance efficiency comparison is conducted to evaluate the performance of the proposed method. In this evaluation, three performance metrics are used numerically to assess the performance efficiency of the suggested control method. The assessment criteria are the

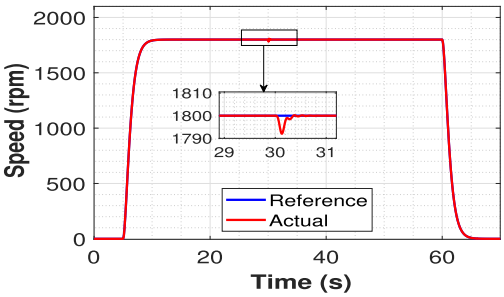

(a) Speed profile

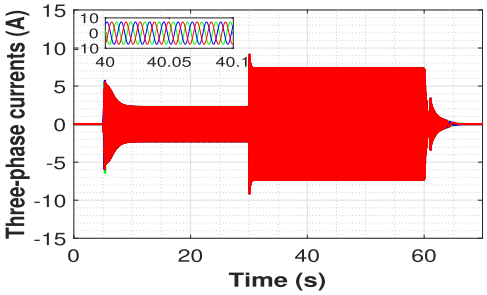

(b) Three phase currents

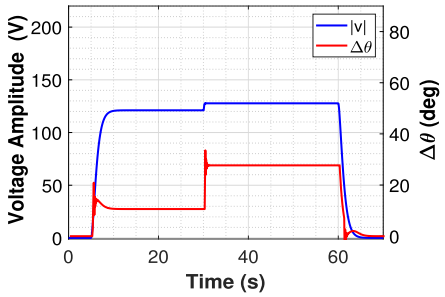

(c) Applied voltage magnitude and angle

FIGURE 11. Evaluation results of the proposed MTPA under friction increase.

integral of absolute speed error (*IAE*), the integral of (*rms*) value of stator current η_s, and the dc-link current integration η_{dc} during the real-time implementation. These metrics are evaluated as follows:

$$IAE = \int_{t_0}^{t_f} |e_\omega| \; dt \tag{25a}$$

$$\eta_s = \int_{t_0}^{t_f} i_{rms} \; dt \tag{25b}$$

$$\eta_{dc} = \int_{t_0}^{t_f} I_{dc} \; dt \tag{25c}$$

The integral bounds t_0 and t_f represent the initial and last time interval.

In addition to the FOC, the obtained numerical values are also compared to the current sensing-based direct voltage MTPA control (DVC) that was proposed in [34], and the outcomes of these evaluations are expressed in Table 3. The first scenario is used for (*IAE*) and η_s evaluation, while the second scenario is used for η_{dc} evaluation. Since the FOC is considered a benchmark, its results are ranked 100%

TABLE 2. Sensitivity evaluation.

Sensitivity S_f^p	$+20\%$	-20%
S_ω^R	0.000382	0.000443
$S_\omega^{L_d}$	0.00246	0.00273
$S_\omega^{L_q}$	0.00324	0.00366
S_ω^λ	0.00781	0.00827

TABLE 3. Performance evaluation.

Criterion	Proposed	DVC [34]	MTPA FOC
IAE	307.23 (88%)	300.32(90%)	273.3 (100%)
η_s	145.19 (96%)	140.07 (97.5%)	139.45 (100%)
η_{dc}	78.93(93%)	76.95 (96%)	73.87 (100%)

efficient. The results obtained from the proposed method and DVC are then expressed in percentages with respect to the benchmark.

It is clear that the numerical values achieved by the proposed method are slightly higher than those of FOC and DVC, which is expected. In this evaluation, the proposed MTPA control method achieved 88%, 96%, and 93% efficiency for *IAE*, η_s and η_{dc}, which are acceptable compared to the FOC. Therefore, the proposed strategy has the ability to track the MTPA trajectory without needing current measurements and regulation loops, with acceptable performance offering simple structure, proper and easy tuning efforts, and fast response to external disturbance, as opposed to the cascaded-based FOC, which highly qualifies it as a substitute for conventional cascaded-based MTPA approaches for low-cost real-time implementation. Considering the current sensing-based DVC, which shows better outcomes, the percentage difference between the proposed method and DVC is only 2%, 1.5% and 3% for *IAE*, η_s and η_{dc} respectively. Compared to DVC, which relies on current measurement for torque estimation, the merits of the proposed technique are apparent in its independence in measured noisy currents and immunity to current sensor failure or misreading. Thus, the reliability of the control system is guaranteed.

Remark: the proposed method currents are only measured for quantitative assessment against the FOC MTPA.

Furthermore, in real-time implementation, computation efficiency plays a vital role in the overall performance of the control system. Hence, code execution time (CET) is selected as a performance metric to evaluate the computation efficiency of the proposed scheme. The findings of the assessment are compared to the conventional MTPA FOC, the dynamic direct voltage control strategy (DDVC) that was proposed in [25], and the current sensing-based simplified dynamic direct voltage control (SDDVC) in [40]. The obtained numerical values are displayed in Table 4.

TABLE 4. Computation efficiency evaluation.

Criterion	Proposed	FOC	DDVC [25]	SDDVC [40]
CET	1.04*ms*	1.25*ms*	1.1*ms*	1.08*ms*

As for the code execution time, the achieved numerical values show that the proposed method requires less time to be executed, with an improvement of 16.8%, 5.45%, and 3.7% against FOC, DDVC, and SDDVC, respectively. This is due to the simplicity of its control design, which eliminates the need for current sensing, transformations, and cascaded regulation, as in the conventional MTPA FOC. Furthermore, the direct calculation of its control laws qualifies it to be faster than the DDVC, whose control signals were obtained based on long-winded iterative calculations.

V. CONCLUSION

MTPA-based field-oriented strategies are commonly used for controlling IPMSMs. As an effort to simplify the control scheme based on cascaded control, a direct voltage control technique was implemented in this study. This strategy avoids the use of current sensing and regulation, offering a simple structure, easier and faster implementation, and less tuning time due to the use of a single-speed controller compared to cascaded-based control systems. The control system also has better reliability because of non-reliance on current sensors. This qualifies it to be a good candidate for cost-effective motor drives, EVs, and large-scale plants, where fast implementation and easy tuning are required. Moreover, the designed strategy provides a complete formulation based on machine voltage equations to derive the MTPA voltage amplitude analytically, disregarding any control law approximation or lookup tables-based numerical solutions. It is relevant to mention that the absence of current measurement and regulation loops leads to a quick response to load torque disturbances. Although the motor's drawn current when using direct voltage control methods is expected to be high, the proposed control strategy has shown its ability to operate the motor with less current consumption for a given load torque. This is because of the proper control of voltage angle. The outcome of this work shows that apart from the simplicity of the proposed control scheme, it has the ability to regulate the speed, especially during the loading period, with acceptable transient performance and current consumption. Lastly, the accuracy of the MTPA trajectory tracking was quantified numerically using performance metrics, and the results reveal an acceptable tracking performance was achieved.

REFERENCES

[1] J. Hang, H. Wu, S. Ding, W. Hua, and Q. Wang, "A DC-flux-injection method for fault diagnosis of high-resistance connection in direct-torque-controlled PMSM drive system," *IEEE Trans. Power Electron.*, vol. 35, no. 3, pp. 3029–3042, Mar. 2020.

[2] J. Hang, H. Wu, S. Ding, Y. Huang, and W. Hua, "Improved loss minimization control for IPMSM using equivalent conversion method," *IEEE Trans. Power Electron.*, vol. 36, no. 2, pp. 1931–1940, Feb. 2021.

[3] C. Lai, G. Feng, K. Mukherjee, J. Tjong, and N. C. Kar, "Maximum torque per ampere control for IPMSM using gradient descent algorithm based on measured speed harmonics," *IEEE Trans. Ind. Informat.*, vol. 14, no. 4, pp. 1424–1435, Apr. 2018.

[4] X. Lin, W. Huang, W. Jiang, Y. Zhao, and S. Zhu, "Deadbeat direct torque and flux control for permanent magnet synchronous motor based on stator flux oriented," *IEEE Trans. Power Electron.*, vol. 35, no. 5, pp. 5078–5092, May 2020.

[5] F. J. Anayi and M. M. A. Al Ibraheemi, "Estimation of rotor position for permanent magnet synchronous motor at standstill using sensorless voltage control scheme," *IEEE/ASME Trans. Mechatronics*, vol. 25, no. 3, pp. 1612–1621, Jun. 2020.

[6] Z. Chen, F. Wang, G. Luo, Z. Zhang, and R. Kennel, "Secondary saliency tracking-based sensorless control for concentrated winding SPMSM," *IEEE Trans. Ind. Informat.*, vol. 12, no. 1, pp. 201–210, Feb. 2016.

[7] X. Liu, H. Chen, J. Zhao, and A. Belahcen, "Research on the performances and parameters of interior PMSM used for electric vehicles," *IEEE Trans. Ind. Electron.*, vol. 63, no. 6, pp. 3533–3545, Jun. 2016.

[8] K. Li and Y. Wang, "Maximum torque per ampere (MTPA) control for IPMSM drives based on a variable-equivalent-parameter MTPA control law," *IEEE Trans. Power Electron.*, vol. 34, no. 7, pp. 7092–7102, Jul. 2019.

[9] T. Sun, J. Wang, and X. Chen, "Maximum torque per ampere (MTPA) control for interior permanent magnet synchronous machine drives based on virtual signal injection," *IEEE Trans. Power Electron.*, vol. 30, no. 9, pp. 5036–5045, Sep. 2015.

[10] T. Shi, Y. Yan, Z. Zhou, M. Xiao, and C. Xia, "Linear quadratic regulator control for PMSM drive systems using nonlinear disturbance observer," *IEEE Trans. Power Electron.*, vol. 35, no. 5, pp. 5093–5101, May 2020.

[11] H. Ge, Y. Miao, B. Bilgin, B. Nahid-Mobarakeh, and A. Emadi, "Speed range extended maximum torque per ampere control for PM drives considering inverter and motor nonlinearities," *IEEE Trans. Power Electron.*, vol. 32, no. 9, pp. 7151–7159, Sep. 2017.

[12] C. Lai, G. Feng, J. Tjong, and N. C. Kar, "Direct calculation of maximum-torque-per-ampere angle for interior PMSM control using measured speed harmonic," *IEEE Trans. Power Electron.*, vol. 33, no. 11, pp. 9744–9752, Nov. 2018.

[13] Q. Chen, W. Zhao, G. Liu, and Z. Lin, "Extension of virtual-signal-injection-based MTPA control for five-phase IPMSM into fault-tolerant operation," *IEEE Trans. Ind. Electron.*, vol. 66, no. 2, pp. 944–955, Feb. 2019.

[14] C. Lai, G. Feng, K. Mukherjee, V. Loukanov, and N. C. Kar, "Torque ripple modeling and minimization for interior PMSM considering magnetic saturation," *IEEE Trans. Power Electron.*, vol. 33, no. 3, pp. 2417–2429, Mar. 2018.

[15] Z. Han and J. Liu, "Comparative analysis of vibration and noise in IPMSM considering the effect of MTPA control algorithms for electric vehicles," *IEEE Trans. Power Electron.*, vol. 36, no. 6, pp. 6850–6862, Jun. 2021.

[16] G. Wang, Z. Li, G. Zhang, Y. Yu, and D. Xu, "Quadrature PLL-based high-order sliding-mode observer for IPMSM sensorless control with online MTPA control strategy," *IEEE Trans. Energy Convers.*, vol. 28, no. 1, pp. 214–224, Mar. 2013.

[17] J. Xia, Y. Guo, Z. Li, J. Jatskevich, and X. Zhang, "Step-signal-injection-based robust MTPA operation strategy for interior permanent magnet synchronous machines," *IEEE Trans. Energy Convers.*, vol. 34, no. 4, pp. 2052–2061, Dec. 2019.

[18] S. Kim, Y.-D. Yoon, S.-K. Sul, and K. Ide, "Maximum torque per ampere (MTPA) control of an IPM machine based on signal injection considering inductance saturation," *IEEE Trans. Power Electron.*, vol. 28, no. 1, pp. 488–497, Jan. 2013.

[19] M. Cheng, F. Yu, K. T. Chau, and W. Hua, "Dynamic performance evaluation of a nine-phase flux-switching permanent-magnet motor drive with model predictive control," *IEEE Trans. Ind. Electron.*, vol. 63, no. 7, pp. 4539–4549, Jul. 2016.

[20] J. Liu, C. Gong, Z. Han, and H. Yu, "IPMSM model predictive control in flux-weakening operation using an improved algorithm," *IEEE Trans. Ind. Electron.*, vol. 65, no. 12, pp. 9378–9387, Dec. 2018.

[21] H. Chaoui, M. Khayamy, and O. Okoye, "Adaptive RBF network based direct voltage control for interior PMSM based vehicles," *IEEE Trans. Veh. Technol.*, vol. 67, no. 7, pp. 5740–5749, Jul. 2018.

[22] Q. Song, S. Zhao, Y. Li, and M. Ahmad, "Voltage vector directional control for IPMSM based on MTPA strategy," *IEEE Access*, vol. 8, pp. 27998–28008, 2020.

[23] H. Chaoui, M. Khayamy, and O. Okoye, "MTPA based operation point speed tracking for PMSM drives without explicit current regulation," *Electric Power Syst. Res.*, vol. 151, pp. 125–135, Oct. 2017.
[24] K. Lee and Y. Han, "MTPA control strategy based on signal injection for V/f scalar-controlled surface permanent magnet synchronous machine drives," *IEEE Access*, vol. 8, pp. 96036–96044, 2020.
[25] M. Alzayed, H. Chaoui, and Y. Farajpour, "Dynamic direct voltage MTPA current sensorless drives for interior PMSM-based electric vehicles," *IEEE Trans. Veh. Technol.*, vol. 72, no. 3, pp. 3175–3185, Mar. 2023.
[26] H. Chaoui, O. Okoye, and M. Khayamy, "Current sensorless MTPA for IPMSM drives," *IEEE/ASME Trans. Mechatronics*, vol. 22, no. 4, pp. 1585–1593, Aug. 2017.
[27] M. Khayamy and H. Chaoui, "Current sensorless MTPA operation of interior PMSM drives for vehicular applications," *IEEE Trans. Veh. Technol.*, vol. 67, no. 8, pp. 6872–6881, Aug. 2018.
[28] P. Haghgooei, A. Corne, E. Jamshidpour, N. Takorabet, D. A. Khaburi, and B. Nahid-Mobarakeh, "Current sensorless control for a wound rotor synchronous machine based on flux linkage model," *IEEE J. Emerg. Sel. Topics Power Electron.*, vol. 10, no. 4, pp. 4576–4586, Aug. 2022.
[29] Z. Chen, Y. Yan, T. Shi, X. Gu, Z. Wang, and C. Xia, "An accurate virtual signal injection control for IPMSM with improved torque output and widen speed region," *IEEE Trans. Power Electron.*, vol. 36, no. 2, pp. 1941–1953, Feb. 2021.
[30] K. Liu and Z. Zhu, "Fast determination of moment of inertia of permanent magnet synchronous machine drives for design of speed loop regulator," *IEEE Trans. Control Syst. Technol.*, vol. 25, no. 5, pp. 1816–1824, Sep. 2017.
[31] M. Moradian, J. Soltani, A. Najjar-Khodabakhsh, and G. R. A. Markadeh, "Adaptive torque and flux control of sensorless IPMSM drive in the stator flux field oriented reference frame," *IEEE Trans. Ind. Informat.*, vol. 15, no. 1, pp. 205–212, Jan. 2019.
[32] M. M. I. Chy and M. N. Uddin, "Development of a nonlinear speed controller of IPMSM drive incorporating MTPA with mechanical parameter estimation," in *Proc. IEEE Int. Electric Mach. Drives Conf.*, May 2007, pp. 322–327.
[33] R. Al-Shehari, H. Chaoui, and H. Gualous, "MTPA trajectory tracking for IPMSM drives: A comparative study and analysis," in *Proc. IEEE Vehicle Power Propuls. Conf. (VPPC)*, Aug. 2018, pp. 1–6.
[34] M. Alzayed and H. Chaoui, "Direct voltage MTPA speed control of IPMSM-based electric vehicles," *IEEE Access*, vol. 11, pp. 33858–33871, 2023.
[35] A. Dianov and A. Anuchin, "Adaptive maximum torque per ampere control of sensorless permanent magnet motor drives," *Energies*, vol. 13, no. 19, p. 5071, Sep. 2020.
[36] R. Dutta and M. F. Rahman, "A comparative analysis of two test methods of Measuring d- and q-axes inductances of interior permanent-magnet machine," *IEEE Trans. Magn.*, vol. 42, no. 11, pp. 3712–3718, Nov. 2006.
[37] Z. Azar, Z. Q. Zhu, and G. Ombach, "Influence of electric loading and magnetic saturation on cogging torque, back-EMF and torque ripple of PM machines," *IEEE Trans. Magn.*, vol. 48, no. 10, pp. 2650–2658, Oct. 2012.
[38] A. Elhaj, M. Alzayed, and H. Chaoui, "Multiparameter estimation-based sensorless adaptive direct voltage MTPA control for IPMSM using fuzzy logic MRAS," *Machines*, vol. 11, no. 9, p. 861, Aug. 2023.
[39] S. Bolognani, L. Peretti, and M. Zigliotto, "Parameter sensitivity analysis of an Improved Open-loop speed estimate forInduction motor drives," *IEEE Trans. Power Electron.*, vol. 23, no. 4, pp. 2127–2135, Jul. 2008.
[40] M. Alzayed and H. Chaoui, "Energy efficiency improvement using simplified dynamic direct voltage maximum torque per ampere control for interior PMSMs," *IEEE/ASME Trans. Mechatronics*, vol. 28, no. 6, pp. 3143–3154, Dec. 2023, doi: 10.1109/TMECH.2023.3256702.

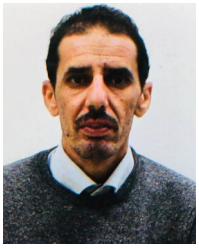

ALAREF ELHAJ received the B.Sc. degree in electrical engineering (automatic control) from the Bright Star University of Technology, Brega, Libya, in 2002, and the M.Sc. degree in automation and control (electrical engineering) from Newcastle University, Newcastle upon Tyne, England, U.K., in 2010. He is currently pursuing the Ph.D. degree in electrical engineering with Carleton University, Ottawa, ON, Canada. He joined the Intelligent Robotic and Energy Systems (IRES) Laboratory, School of Engineering, Carleton University, in January 2020. His research interest includes the modeling and control of permanent magnet synchronous motors.

MOHAMAD ALZAYED (Member, IEEE) received the Ph.D. degree in electrical power engineering, in 2011. His career has bridged both academia and industry with more than 14 years of experience in control and electrical energy resources, grid management and efficiency, electrical design and contracting, and project management. He has sound knowledge of renewable energy, smart systems, SCADA and BMS design and programming systems, industrial control, and automation. Since 2019, he has been a member of the Intelligent Robotic and Energy Systems Research Group, Department of Electronics, Carleton University, Ottawa, ON, Canada. His teaching experiences include energy distribution and efficient utilization, sustainable energy systems, power systems and control, electric machines, and power electronics. His research interests include developing intelligent algorithms for the control of electric machines and power electronic converters for wind renewable energy systems, real-time simulations, and storage applications. He is the guest editor of various journals.

HICHAM CHAOUI (Senior Member, IEEE) received the Ph.D. degree (Hons.) in electrical engineering from the University of Quebec, Trois-Rivières, QC, Canada, in 2011.

His career has spanned both academia and industry in the field of control and energy systems. From 2007 to 2014, he held various engineering and management positions with Canadian industry. He is currently an Associate Professor with Texas Tech University, Lubbock, TX, USA, and Carleton University, Ottawa, ON, Canada. His scholarly work has resulted in over 200 journals and conference publications. His research interests include adaptive and nonlinear control theory, intelligent control, robotics, electric motor drives, and energy conversion and storage systems. He was a recipient of the Best Thesis Award, the Governor General of Canada Gold Medal Award, the Carleton's Faculty of Engineering and Design's Research Excellence Award, the Early Researcher Award from the Government of Ontario, and the Top Editor Recognition from IEEE Vehicular Technology Society. He is a Registered Professional Engineer in the Province of Ontario. He is also an Associate Editor of IEEE TRANSACTIONS ON POWER ELECTRONICS, IEEE TRANSACTIONS ON VEHICULAR TECHNOLOGY, IEEE TRANSACTIONS ON AUTOMATION SCIENCE AND ENGINEERING, and several other journals.